https://doi.org/10.5194/essd-2019-171
Preprint. Discussion started: 17 October 2019

Open Access Earth System Science Data Discussions

A coastally improved global dataset of wet tropospheric corrections for satellite altimetry

Clara Lázaro[1,2], Maria Joana Fernandes[1,2], Telmo Vieira[1,2], Eliana Vieira[1]

[1]Faculdade de Ciências, Universidade do Porto, 4169-007 Porto, Portugal
[2] Centro Interdisciplinar de Investigação Marinha e Ambiental (CIIMAR/CIMAR), Universidade do Porto, 4050-123 Porto, Portugal

Correspondence to: Clara Lázaro (clazaro@fc.up.pt)

Abstract. Global mean sea level is a valuable proxy to understand climate change and how it operates, since it includes the response from various components of the climate system. Global sea level rise is accelerating, which is a concern for coastal areas management from medium to long-term time scales. Satellite radar altimetry (RA) has been providing us information regarding the sea level anomaly (SLA) field and its space-time variability since the early 90s. As satellite orbit determination, reference surfaces (e.g., mean sea surface) and instrumental, range and geophysical corrections improved over the decades, the data from past missions were reprocessed subsequently, leading to an SLA dataset over open ocean accurate to the centimetre-level. The accuracy of satellite altimetry is known to deteriorate towards the coastal regions due to several reasons, amongst which the improper account for the wet path delay (WPD) can be pointed out. The most accurate WPDs for RA are derived from the on-board microwave radiometer (MWR) radiance measurements, acquired simultaneously as the altimeter ranges. In the coastal zone, however, the signal coming from the surrounding land contaminates these measurements and the water vapour retrieval from the MWR fails. As meteorological models do not handle coastal atmospheric variability correctly yet, the altimeter measurements are rejected whenever MWR observations are absent or invalid. The need to solve this altimetry issue in the coastal zone, simultaneously responding to the growing demand of data in these regions, motivated the development of the GNSS-derived Path Delay (GPD) algorithm.

The GPD combines WPD from several sources through objective analysis (OA) to estimate the WPD or the corresponding RA correction accounting for this effect, the wet tropospheric correction (WTC), for all along-track altimeter points for which this correction has been set as invalid or is absent. The current GPD version (GPD Plus, GPD+) uses as data sources WPD from coastal and island GNSS stations, from satellites carrying microwave radiometers, and from valid on-board MWR measurements. The GPD+ has been tuned to be applied to all, past and operational, RA missions, with or without an on-board MWR. The long-term stability of the WTC dataset is ensured by its inter-calibration with respect to the Special Sensor Microwave Imager (SSM/I) and SSMI/I Sounder (SSM/IS). The dataset is available for TOPEX/Poseidon (T/P), Jason-1 and Jason-2 (NASA/CNES), Jason-3 (NASA/EUMETSAT), ERS-1, ERS-2, Envisat and CryoSat-2 (ESA), SARAL/AltiKa (ISRO/CNES) and GFO (U.S. Navy) RA missions. The GPD+ WTC for Sentinel-3 shall be released soon. The present paper describes the GPD+ database and its independent validation through statistical analyses of SLA. Overall, results show that the

https://doi.org/10.5194/essd-2019-171
Preprint. Discussion started: 17 October 2019

Open Access Earth System Science Data Discussions

GPD+ WTC is the most effective in reducing the SLA variance in the coastal regions, in particular for the ESA missions. Moreover, GPD+ recovers a significant number of measurements, which otherwise would be rejected due to land, rain and ice contamination and instrument malfunctioning. Consequently, GPD+ database has been chosen as reference WTC in the Sea Level Climate Change Initiative (CCI) products; the GPD+ has also been adopted as reference in CryoSat-2 Level 2 Geophysical Ocean Products (GOP). Strategies to further improve the methodology, therefore enhancing the quality of the database, are also discussed. The GPD+ dataset is archived on the homepage of the Satellite Altimetry Group, University of Porto, publicly available at the repository https://doi.org/10.23831/FCUP_UPORTO_GPDPlus_v1.0 (Fernandes et al., 2019).

1 Introduction

Since the early 1990s, satellite radar altimetry (RA) missions have been observing the oceans, measuring global and regional mean sea level, as well as its change. Altimeters on board RA missions measure the sea surface height (SSH) by subtracting the measured altimeter range, the nadir-measured distance between the satellite and the sea surface, from the satellite altitude (H) above a reference ellipsoid of a terrestrial (geocentric) reference frame, currently known with a centimetre-level radial error. In the computation of precise SSH, a multitude of well understood effects must be properly considered: those that introduce errors in the measured range, e.g. atmosphere propagation delay, and those that induce SSH variability other than that under analysis over time, e.g. ocean tides and atmospheric pressure. Sea surface height anomalies, or sea level anomalies (SLA), are computed subtracting a mean sea surface (MSS) from the corrected SSH measurements.

Range corrections are required to account for the delay the microwave pulses suffer, as they propagate through the atmosphere (ionospheric and tropospheric corrections, the latter including the effect of the neutral atmosphere) and for the interaction with the sea surface (sea state bias); geophysical corrections account for the sea level variability due to tides (ocean, solid earth and polar tides, as well as loading effects) and for the ocean's response to atmospheric pressure (dynamic atmospheric correction, a combination of a high-frequency signal with the low-frequency inverted barometric response of the ocean); if needed to homogenize and inter-calibrate multi-mission data, the reference frame offset correction is applied, accounting for instrument-dependent effects and biases between missions (Fernandes et al., 2014). A detailed description of the corrections is given in Chelton et al. (2001).

This may be expressed as:

$$SLA = H - R_{corr} - MSS \quad (1)$$

where R_{corr} is the altimeter range (R) corrected for all instrument (ΔR_{inst}), range (ΔR_{range}) and geophysical (ΔR_{geoph}) effects:

$$R_{corr} = R + \sum(\Delta R_{range} + \Delta R_{geoph} + \Delta R_{inst}) \quad (2)$$

The quality of the SLA measurements has considerably improved over time, essentially because new models and corrections have become available, and satellite orbit determination as well as radar processing has improved in absolute accuracy. This

https://doi.org/10.5194/essd-2019-171
Preprint. Discussion started: 17 October 2019

is particularly true over open ocean, where altimeter waveforms do not depart from the expected shape given by the Brown model and geophysical and range corrections can be accurately estimated (Chelton et al., 2001, Fernandes et al., 2006).

The total tropospheric path delay for microwaves can be divided into two components, one depending only on the surface pressure, the hydrostatic term, and a remainder that mainly depends on water vapour abundance, commonly termed wet path delay (WPD) (Askne and Nordius, 1987). The dry tropospheric correction (DTC) accounts for the hydrostatic term that, despite having an absolute value as large as 2.3±0.2 m in the zenith direction at sea level, can be calculated with millimetre-accuracy, provided the surface atmospheric pressure is known at each location (Fernandes et al., 2014). From here onwards, the terms DTC and WTC are used to refer to the dry and wet tropospheric corrections (negative values), respectively, applied to RA measurements and, accordingly, DPD and WPD to the corresponding absolute values. The DTC computation can be carried out using sea level pressure fields given by numerical weather models (NWMs), as described e.g. in Fernandes et al. (2013a). Ranges are corrected for the wet path delay through the wet tropospheric correction (WTC), possessing an absolute value less than 0.50 m. Contrasting to the estimation of the DTC, the WTC retrieval requires the knowledge of the full water vapour and temperature profiles, which are known to be highly variable, both temporally and spatially (Dousa and Elias, 2014; Vieira et al., 2019a). Therefore, to properly account for the microwave propagation delay through the troposphere, RA missions carry aboard a passive microwave radiometer (MWR), nadir-looking instruments capable of measuring both the water vapour and the cloud liquid water components of the wet path delay, from brightness temperatures in appropriate bands of the microwave spectrum.

Radiometers embarked on RA missions can be divided into two main groups (Steunou et al., 2014). Two-channel MWR, operating at frequencies 21–23.8 GHz, the primary water vapour sensing channel, and 34–37 GHz, carried by the European Space Agency (ESA) ERS-1, ERS-2 and Envisat, by ESA/EUMETSAT Sentinel-3, and by US Navy's mission Geosat Follow-On (GFO) and by the joint Indian Space Research Organization (ISRO) and Centre National d'Études Spatiales (CNES) SARAL (Satellite with ARgos and ALtiKa) missions; three-channel MWR carried by NASA's missions TOPEX/Poseidon (T/P), Jason-1, Jason-2 and Jason-3, with an additional channel operating at 18–18.7 GHz. MWR footprints vary in the range of from 20 to 45 km, depending on the instrument and frequency except for the one embedded within SARAL's altimeter, for which the dual frequency radiometer has a footprint of diameter less than 12 km (Steunou et al., 2014).

Accurate measurements of the integrated amount of water vapour and cloud liquid in the atmosphere are achievable in open ocean, but difficult to perform in coastal regions where the precise modelling of the WTC is still challenging. Nearly a decade ago, the RA community started developing new algorithms and methodologies aiming at recovering altimetric data in the coastal region, leading to a more mature status of the emerging, at that time, field of coastal altimetry. Altimetric data in the closest 50 km away from the coast are usually flagged as invalid, being therefore discarded, or non-existent due to several reasons. On the one hand, the shape of the waveforms no longer can be described by the Brown model and this is overcome using specific retracking techniques; on the other hand, the accurate modelling of some corrections is difficult. This is particularly true for the estimation of the wet path delay, and consequently of the WTC, since in coastal areas the measurements of the MWR are in general contaminated by land, in part due to the large diameter of its footprint. Also important, is the fact

https://doi.org/10.5194/essd-2019-171
Preprint. Discussion started: 17 October 2019

that the WTC retrieval algorithms are designed for open-ocean conditions, thus assuming surface emissivity values only valid for the open-ocean case; however, surface emissivity can be highly variable when the surrounding land surfaces contribute partially to the returning signal, causing a failure of the retrieval algorithms. Different strategies have been proposed in the last years to accomplish the estimation of the wet tropospheric correction in coastal areas, which are summarized in Cipollini et al. (2017). One of these is the GNSS (Global Navigation Satellite System) derived Path Delay (GPD) algorithm. The GPD was developed by the University of Porto (UPorto) in the scope of the ESA's funded project COASTALT (Vignudelli et al., 2009) to estimate the WTC for correcting the altimetric data in the coastal European region. It has evolved over the last years reaching a mature status recently (GPD Plus, GPD+), with the global computation of a WTC dataset for all operational and past RA missions that has been adopted as reference to derive the ESA Climate Change Initiative Sea Level dataset (Quartly et al., 2017, Legeais et al., 2018). The aim of this study is to describe and grant access to the GPD+ collection of WTCs for RA provided by UPorto (Fernandes et al., 2019). Results regarding the validation of this dataset are shown for the recently reprocessed and released Envisat Geophysical Data Records (GDR) V3.0 dataset, for which the GPD+ shows a substantial improvement in the computation of the SLA dataset over coastal and polar regions. For more results, readers may refer to Fernandes et al. (2015) and Fernandes and Lázaro (2016, 2018).

2 The GPD+ algorithm and the GPD+ WTC database

The main objective of the GPD+ algorithm is the estimation of the WTC for coastal regions, where MWR-derived WPDs, if available, are usually invalid values due to land contamination both in the altimeter and MWR observations. If uncorrected, this leads to a rejection of a large number of points in these regions. To accomplish this task, WPD datasets from different sources are combined through an optimal interpolation scheme. The input data are described in Sect. 2.1, the technical description of the algorithm is presented in Sect. 2.2 and the generated WTC database in Sect. 2.3.

2.1 Input WPD observations

In the most recent version of the algorithm, WPDs from the following sources are used as input: 1) tropospheric zenith total delays (ZTDs) computed at a dense GNSS network of stations distributed globally along the coastline; 2) total column water vapour (TCWV) products generated from measurements from passive imaging MWR on board environmental and meteorological Earth observation satellites; 3) along-track WTC (the symmetric of WPD) measurements from the on-board MWR, before they become invalid when approaching coast. The algorithm also provides valid WTC estimates for offshore and open-ocean measurements for which invalid WTC are detected, provided WPD observations are available at those geographical locations. This way, the algorithm attempts to eliminate measurements contaminated by heavy rain and ice, as well as faulty measurements due to, e.g., instrument malfunctioning.

https://doi.org/10.5194/essd-2019-171
Preprint. Discussion started: 17 October 2019

125 **2.1.1 WPD from GNSS-derived ZTD**

Tropospheric propagation delays are a source of error in GNSS positioning as well, being therefore estimated, at each GNSS station, for each observation. The quantity computed at each station is the slant total delay (STD) between the satellite and the ground-based station. Provided *a priori* value for the zenith hydrostatic delay (ZHD or DTC in satellite altimetry terminology), computed from knowledge of surface atmospheric pressure either measured locally or NWM-derived meteorological data, and
130 mapping functions for hydrostatic and wet components are known, the ZTD at station height can be computed with millimetre accuracy (Pany et al., 2001, Fernandes et al., 2013a, 2015). Mapping functions relate the delay in the station zenith direction, ZTD, with that in the actual satellite-station direction, STD. While the wet delay varies in time in an unpredictable way, the ZHD can be derived with millimetre accuracy from e.g. NWMs (Pany et al., 2001). Therefore, an *a posteriori* more accurate ZHD can be computed and subtracted from the estimated ZTD, yielding the wet delay in the zenith direction (zenith wet delay,
135 ZWD or WPD in satellite altimetry terminology). ZHDs, computed with millimetre accuracy at station height from ZHDs at sea level derived from sea level pressure (SLP) fields from an NWM (e.g. ERA Interim or ECMWF operational) and further reduced to station height using an adequate height reduction procedure, are used to derive WPD from GNSS (Fernandes et al., 2013a, 2015). The WPD obtained this way are given at station height and therefore at a level different from that of interest in satellite altimetry, which is the mean sea level. Therefore, the height reduction of the WPD is required. This has been performed
140 using an exponential decay function, empirically obtained by Kouba (2008), valid for WPD height reductions for heights below ~1000 m (Vieira et al., 2019b).

This summarises the methodology adopted by UPorto in the computation of WPD from GNSS measurements. A complete description of the methodology and its assessment can be found in Fernandes et al. (2013a, 2015) or Vieira et al. (2019b). Zenith total delays (ZTD) estimated at UPorto, along with those available online from international GNSS services (IGS
145 (International GNSS Service), EPN (EUREF Permanent Network) and SuomiNet) and from several stations located at the German Bight, provided to UPorto by the Technische Universität Darmstadt (TUD) in the scope of ESA's Climate Change Initiative (CCI) project, have been used. More than 800 coastal (at distances from the coast less than 100 km) and offshore GNSS stations, with altitude below 1000 m, are being used at the time of writing. Figure 1 shows, for the Envisat period, the increase both in the number of GNSS stations and GNSS observations used as input in the GPD+ algorithm. The number of
150 stations almost duplicates, in 2008.5, relatively to the number of stations in the beginning of the period and have been continuously increasing until present.

2.1.2 WPD from scanning imaging MWR

The methodology developed by UPorto to calculate the WTC from TCWV products from passive imaging MWR on board Earth observation satellites is discussed in detail in Fernandes et al. (2013b, 2015). These data are of extreme importance for
155 use in the GPD+ since they provide the unique possibility of computing the WTC over open ocean for those RA missions that

https://doi.org/10.5194/essd-2019-171
Preprint. Discussion started: 17 October 2019

do not possess an MWR, like e.g. CryoSat-2. In fact, GPD+ is an upgrade from the GPD methodology, which was developed to compute the WTC only for coastal points, thus relying only on GNSS and valid on-board MWR measurements.

TCWV datasets from 20 scanning imaging (SI) passive MWR, available at NOAA Comprehensive Large Array-Data Stewardship System (CLASS) and at Remote Sensing Systems (RSS) have been selected. CLASS includes data from the AMSU-A (Advanced Microwave Sounding Unit-A) on board NOAA-16, -17, -18, -19, MetOp-A and MetOp-B satellites. RSS delivers datasets for several sensors, namely SSM/I (Special Sensor Microwave Imager) and SSM/IS (SSM/I Sounder) on board DMSP (Defense Meteorological Satellite Program) satellites (F08, F10, F11, F13, F14, and F16, F17, F18, respectively), WindSat aboard Coriolis, Tropical Rainfall Measuring Mission's (TRMM) radiometer TMI (TRMM Microwave Imager), Global Precipitation Measurement's (GPM) Microwave Imager (GMI), AMSR-E (Advanced Microwave Scanning Radiometer for EOS) on board AQUA and AMSR-2 in the Japanese Global Change Observation Mission – Water Satellite 1 (GCOM-W1). Table 1 shows the availability of the TCWV products used as input in GPD+.

For the Envisat mission, for example, the number of SI-MWR increased from 4 to 11, from the beginning (2002) to the end (2012) of the mission, respectively.

The calculation of the path delay from TCWV can be performed knowing that the quotient between WPD and TCWV is modelled by a decreasing function of WPD of the type

$$\frac{WPD}{TCWV} = a_0 + a_1 TCWV + a_2 TCWV^2 + a_3 TCWV^3 \quad (3)$$

with constants a_0 = 6.8544, a_1 = −0.4377, a_2 = 0.0714, and a_3 = −0.0038, for TCWV in the right-hand side of the equation in centimetres (Stum et al., 2011).

It is known that, in addition to TCWV, WPD also depends on temperature. Expressions such as Eq. (3) account for an implicit modelling of this dependence. Fernandes et al. (2013b) have shown that this expression leads to similar results as those obtained by adopting formulae that make use of explicit values of atmospheric temperature given e.g. by an NWM.

2.1.3 WPD from along-track MWR

The provenience of the MWR-derived WTC used as input in the GPD+ is the Radar Altimeter Database System (RADS) (Scharroo et al., 2012), except for Envisat, as this mission has been recently reprocessed. We recall that the WTC is the symmetric of the wet path delay and the quantity of interest in satellite altimetry. RA data necessary to compute the SLA datasets used to validate the GPD+ WTC are also extracted from RADS. For each RA mission, only valid MWR-derived WTC are input in the algorithm, therefore the correct identification of valid/invalid measurements is of crucial importance. Exception made for CryoSat-2 (for which, in the absence of an on-board MWR, a WTC is generated for all along-track altimeter points), GPD+ estimates a WTC for those points with an invalid MWR-derived WTC only. In this way, the valid observations from the on-board MWR are preserved.

Invalid measurements are usually detected using a set of flags, some of them provided in the products, as the radiometer flag for the surface type or the ice flag. If different from 0, these flags indicate invalidity due to land contamination or instrument

https://doi.org/10.5194/essd-2019-171
Preprint. Discussion started: 17 October 2019

malfunctioning, or ice, respectively. MWR-derived WTCs outside the range -0.5 m ≤ WTC <0.0 m, generally due to heavy rain or ice, are also discarded. A validity criterion based on the distance from coast is also applied: if the location of a certain MWR measurement is such that its distance from the coast is less than a threshold value, then this measurement is most certainly contaminated by land. Threshold values used in this criterion depend on the RA mission. Adopted values are based on the known characteristics of each instrument and on an independent assessment of the on-board MWR observations using GNSS-derived WPDs in the coastal zones (Vieira et al., 2019b). Results for ESA missions are alike, showing that land contamination occurs at distances from coast less than 30 km; the same threshold has been used for GFO and T/P. In relation to the remaining NASA missions, values of 15 km have been used for Jason-1/2/3. For SARAL, a threshold value of 15 km was adopted. Also, noisy MWR measurements are discriminated using median filters based on statistical analysis of the differences to the NWM-derived WTC on the same along-track point and neighbouring points. Invalid measurements are detected if: 1) radiometer surface type flag is different from 0; 2) ice flag different from 0; 3) do not satisfy the defined statistical criteria or are outside WTC limits, 4) are at a distance from coast less than the threshold established for that mission. Figure 2 shows all the along-track points flagged as invalid for Envisat cycle 12. As it will be shown in Sect. 3 for Envisat, per cycle and on average, approximately 30% of the oceanic points have an invalid WTC value; for these points, an SLA value cannot be computed due to the invalidity of the WTC or of other corrections, or because certain criterion is not met (e.g., number of 18 Hz measurements to compute the 1 Hz values used less than the imposed minimum). For approximately 10% of all oceanic points, the WTC is the only correction that prevents the computation of the SLA. This is, on average, the percentage of points with a valid SLA value recovered by the GPD+ algorithm for a mission such as Envisat.

2.1.4 Radiometer Calibration

Uncertainty in sea level rise quantification is required by the Global Ocean Observing System to be under 0.3 mm/year. To ensure long-term stability of the GPD+ WTC, the large set of radiometers used in this study have been previously inter-calibrated through the inter-comparison of the various datasets. Data from the reference missions have been calibrated against those of the Special Sensor Microwave Imager (SSM/I) and the SSM/I Sounder (SSM/IS) by selecting matching points from each pair of missions operating simultaneously with a difference in time and location less than 45 minutes and 50 km, respectively (Fernandes et al., 2013b). The time-series of these matching points was used with a 3-parameter model to adjust offset (a), scale factor (b) and linear trend (c) for each mission (Fernandes and Lázaro, 2016):

$$Y = a + bX + c(T - T_0), \;\; T_0 = 1992 \tag{4}$$

The remaining altimetry missions were then inter-calibrated to these calibrated datasets from the reference missions since orbits of most all remaining missions are sun-synchronous with different times for the Equator crossing than those of the SSM/I(S), with a small number of matchups mostly found at high latitudes, not representative of the WTC variability. For these missions, data were analysed at crossover points and the same adjustment parameters were obtained from the time-series. For the crossover analysis, only data with difference in time less than 180 minutes were used. As an example, the calibration

https://doi.org/10.5194/essd-2019-171
Preprint. Discussion started: 17 October 2019


Open Access Earth System Science Data Discussions

parameters have been obtained for Envisat are a=-6.82 mm; b=0.991 and c=-0.0028 mm/yr, showing that the trend is negligible and indicating that the dataset is well aligned with the altimeter reference missions and with SSM/I and SSM/IS. The small offset and scale factor have the impact of making the correction more negative by 6-7 mm.

2.1.5 WPD from NWM

Space-time collocated WTCs from NWM grids are adopted in the OA as first guess. Usually the European Centre for Medium range Weather Forecasts (ECMWF) ReAnalysis (ERA) Interim model, provided each 6 hours with 0.75° × 0.75° spatial resolution, is used for missions prior to 2004. For missions after this period, the ECMWF Operational Model (ECMWF Op., 6-hour time interval, 0.125° × 0.125° spatial resolution) is selected. Therefore, in the absence of observations to improve the first guess, a WTC estimate from ERA Interim or ECMWF Op. is output from GPD+. This is normally the case for the northernmost latitudes. In addition, to reduce data discontinuities, output values solely based on model data are adjusted to the valid MWR measurements of each cycle by solving for the mean difference between the two datasets.

2.2 Algorithm description

The GPD+ algorithm is based on objective analysis and estimates the wet path delay, given measurements from different sources of the variable under study at a restricted number of data points. The statistics of the field are estimated in the form of a correlation function and of the measurement errors associated with each type of observation. The expected error associated to this estimate is also derived. The technique for the objective analysis is fully described in Bretherton et al. (1976).

The algorithm has been originally implemented to calculate the WTC in the coastal zone, where the retrieval of the wet path delay from on-board MWR measurements become invalid. Later, it has evolved to provide the correction also over open ocean, providing the correction during, for example, instrument malfunctioning, and inland waters.

For all satellite missions but CryoSat-2 and for each along-track point deemed as invalid, a WTC estimate is calculated from valid WTC observations from different sources at the nearby location and within a time interval, defined by the spatial and temporal radiuses of influence used in the computation. In the current GPD+ version, these radiuses have been set equal to the correlation spatial and temporal scales. Whilst the spatial correlation scale varies spatially, both with longitude and latitude (Fernandes and Lázaro, 2016), the temporal correlation scale has been set to 100 minutes (Bosser et al., 2007). For the CryoSat-2 mission, since it does not carry a passive microwave radiometer, a GPD+ WTC estimate is computed for every along-track point using third-party data only. The location and time of each along-track are those provided in the GDR products present in RADS. Due to the temporal difference between adjacent satellite tracks, in practice only along-track valid MWR measurements from the track to which the point of estimation belongs are used.

Regarding the accuracy of the observations, a constant value of 0.5 cm has been set for the white noise of the GNSS- and MWR-derived wet path delays, while for the SI-MWR observations a value between 0.7 cm and 1.1 cm, depending on the mission, has been used (Fernandes et al., 2013b).

https://doi.org/10.5194/essd-2019-171
Preprint. Discussion started: 17 October 2019

The procedure for finding a good estimate of the WTC starts with the definition of the first guess or *a priori* value for the field. In the current version of the algorithm, the first guess is the space-time collocated NWM-derived wet path delay from ERA Interim or ECMWF-Op, the most suitable depending on purpose and time period. Therefore, in the absence of observations, the GPD+ WTC equals the NWM-derived WTC. In the presence of observations, its input number is limited to 15 in order to decrease computational burden; the chosen observations are those for which the statistical weights are larger, meaning that for these measurements the differences in acquisition time and distance to the point where the estimate is being calculated are the smallest.

The estimates for those missions that embark an MWR rely on the valid MWR-derived WPD values. Therefore, one of the core competencies of the GPD+ methodology is its ability to detect corrupted WTC values, which is achieved through the definition of improved criteria for their detection. Measurements flagged as invalid are those that: -have the radiometer surface type flag set as 1; - are contaminated by ice; - are contaminated by rain; - are outside the range [-0.5 m, 0.0 m]; have mission-dependent flags (e.g., radiometer along-track averaging flag for Envisat) set as 1; - do not satisfy several statistical criteria based on the differences between adjacent measurements and between MWR and NWM values; - are at distances from coast less than 15 or 30 km, depending on being a reference and SARAL or ESA mission.

A general Gaussian space-time correlation function of the form

$$G(r,\Delta t) = e^{-\frac{r^2}{C^2}}.e^{-\frac{\Delta t^2}{T^2}} \quad (5)$$

where r and Δt represent the distance and the time interval between acquisitions of each pair of points, and C and T are the spatial and temporal correlation scales, respectively, has been adopted to account for the spatial and temporal variability.

A diagram showing the workflow of the GPD+ algorithm is shown in Fig. 3.

2.3 GPD+ WTC files description and nomenclature

As the impact of the correction is mainly in ocean studies, in the current version, the final GPD+ WTCs are continuous products over the ocean and coastal regions. To prevent the loss of points when interpolating to 20 Hz points, in addition to ocean points, the closest land point is included, provided it is within a distance less than 50 km from the ocean. For Envisat, as this mission has been recently reprocessed (Version 3.0), the GPD+ WTC covers the whole range of latitudes and surfaces, including land. Corrections are currently publicly available for ten RA missions: T/P, Jason-1, Jason-2, Jason-3, GFO, ERS-1, ERS-2, Envisat, SARAL and CryoSat-2. Figure 4 gives an example of the GPD+ WTC for Envisat's cycle 12, showing global coverage (top panel) and over ocean regions with valid sea level anomaly values (bottom panel). As stated above, the correction has its main impact over the ocean since it is meant to be used to improve satellite altimetry. Over non-oceanic surfaces, the correction has been set equal to the ECMWF ERA Interim or Operational models, depending on the mission, as previously explained (Sect. 2.1.5). As already done for Envisat, future versions of the correction will cover all surface types for all missions. In addition,

https://doi.org/10.5194/essd-2019-171
Preprint. Discussion started: 17 October 2019

over non-oceanic regions where WPD observations exist (e.g. from MWR over large lakes or from GNSS), new estimates will be obtained based on available measurements.

The GPD+ WTC products, which content is described in Table 2, are provided for each cycle of the mentioned altimetric missions. For the time and location of each altimeter measurement, specified by the variables 'time_01' in UTC seconds since 2000-01-01 00:00:00.0 and 'geodetic lat_01' and 'lon_01' in degrees as given in each GDR file, the GPD+ wet tropospheric correction, in metres, and its associated validity flag, fields 'GPD_wet_tropo_cor_01' and 'GPD_wet_tropo_cor_qual_01' respectively, are provided at 1 Hz. The sign convention adopted is that the WTC should be added to the range measured by the altimeter to correct it for the range delay. The data-quality flag can take the following values:

- 0: the MWR-derived WTC is valid and, in this case, the GPD+ correction is equal to the MWR-derived WTC, after applying calibration factors, therefore preserving the high accuracy of these data;
- 1: the invalid MWR-derived WTC has been replaced by a valid GPD+ estimate based on observations;
- 2: no observations were available for the computation and the GPD+ estimate is the first guess (i.e., ERA Interim for TOPEX/Poseidon, ERS-1, ERS-2, Envisat, Jason-1 or ECMWF Op. for OSTM/Jason-2, Jason-3, Cryosat-2, SARAL/AltiKa) with possible small bias applied.
- 3: GPD + estimate is outside the valid range ([-0.5, 0.0]), and either the value -0.5 or 0.0 was attributed to the output value.

By using this flag, a knowledgeable user can select the data most suitable for a given application: a continuous correction e.g. for coastal studies, solely the valid measurements for the on-board MWR (e.g. for calibration purposes or global climate studies) or exclude the points solely based on NWM values.

NetCDF files include self-documenting variables and common attributes.

The nomenclature selected for the GPD+ dataset is:

< MISSION>_c<CYCLE_NUMBER>_gpd.nc

where <MISSION> is two-letter code that depends on the mission (see Table 3) and <CYCLE_NUMBER> is a three-digit number indicating the cycle number of <MISSION>. In all cases, the RADS cycle number convention has been adopted. In cases such as Jason-1 geodetic phase (phase c), cycle numbers are different from those adopted by AVISO. For CryoSat-2, sub-cycle numbers of 27 or 29 days are used according to RADS convention. The availability of GPD+ WTC for each mission is presented in Table 3 (Fernandes et al., 2019).

3 Results and Discussion

Results here provided have been obtained in the scope of several ESA-funded research projects and present new scientific findings that have not been published before. For Envisat, the GPD+ WTC was computed for inclusion in the newly reprocessed Envisat Geophysical Data Records (GDR) V3.0 in the ambit of the ESA second Envisat Altimetry Full Mission Reprocessing (FMR).

https://doi.org/10.5194/essd-2019-171
Preprint. Discussion started: 17 October 2019

For results concerning the remaining satellite altimetry missions the reader is advised to consult Fernandes and Lázaro (2018) for Sentinel-3, Fernandes and Lázaro (2016) for Cryosat-2 and GFO, and Fernandes et al. (2015) for T/P, Jason-1 and -2 and ESA missions, however the latter results were obtained with a previous version of GPD+, the so-called GPD algorithm.

3.1 GPD+ WTC for Envisat Mission

Results for Envisat cover the period May 2002 to April 2012, cycles 6 to 113, which corresponds to the whole dataset released in July 2018 (ESA, 2019). The GPD+ WTC is here compared to the ECMWF Reanalysis WTC (ERA Interim, GDR field mod_wet_tropo_cor_reanalysis_01) and with the WTC present in the AVISO CORSSH L2P products in July 2019 (AVISO, 2017). The latter dataset is usually called Composite Correction since, as GPD+, also combines original MWR values with those from models, in the regions where the former are invalid (Mercier, 2004; Mercier et al., 2010). The main difference between GPD+ and the Composite WTCs is that the first estimates the new WTC values from observations (whenever available) while the second uses only NWM-derived WTCs, previously adjusted to the closest valid MWR.

This FMR follows the first Envisat Altimetry reprocessing Version (V2.1) completed in 2012 (ESA, 2018). The Envisat V3.0 reprocessed data have been improved, comparatively to the previous version, in many aspects, among which is an increased availability of the data acquired by the MWR, particularly at the beginning of the mission.

In the estimation process, the ERA Interim WTC was selected as first guess, being therefore the adopted values in the absence of measurements, as those occurring over land. Anomalies in this field have been found, with the field out of limits in a set of points, most of them concentrated on certain passes, making it unsuitable for use in the GPD+ estimations. To be able to use the ERA Interim WTC, abnormal values present in the products were replaced by those computed from single layer fields of TCWV and 2-metre temperature, with the formulation used by Fernandes and Lázaro (2016).

The MWR-based correction used in the generation of these files is the 'rad_wet_tropo_cor_sst_gam_01' GDR field, hereafter called ‘on-board MWR-derived WTC’. Figure 5 shows the GPD+ WTC for some Envisat tracks, exemplifying several issues commonly encountered in the on-board MWR-derived WTC that no longer exist in the GPD+ WTC: unavailability of the correction; correction contaminated by ice; existence of outliers; and correction contaminated due to land proximity. It is important to refer that the corrections are shown only for points for which a valid SLA value can be computed after recovering the WTC, as explained in what follows.

Figure 6 summarizes, for the whole Envisat period (cycles 06 to 113), interesting results. The percentage of points, for each Envisat cycle, with a rejected MWR-derived WTC, for which a GPD+ estimate has been computed are represented in pink and are seen to be around 30%. The corresponding percentage of points for which a valid SLA value could be computed after the estimation of the WTC by the GPD+ is shown in green. The number of points with valid SLA values (in grey) per cycle is also represented. This figure allows us to show that the GPD+ algorithm leads to the recovery of approximately 10% of the points with valid SLA value. In some cycles this value can reach 20% or more, most of these points are located at high latitudes and in coastal regions. Keeping in mind that ESA missions are near-polar missions with an inclination of ~98.5º, they have the great advantage, when compared to the reference missions, of acquiring measurements at high latitudes. The recovery of data

https://doi.org/10.5194/essd-2019-171
Preprint. Discussion started: 17 October 2019

in these regions, besides along the coastal regions, can be considered one of the greatest advantages of the GPD+ methodology. The given figures show that for around 20% of the altimeter measurements, an SLA value could not be computed due to a reason other than the invalidity of the WTC. This means that if in future FRM the issues that prevent the SLA computation are totally or partially solved, the percentage of data recovery will increase up to a maximum of 30% when the GPD+ WTC is used. Despite being provided continuously, the GPD+ WTC has its largest impact over ocean.

GNSS data cannot be considered independent from the GPD+ WTC, since they have been used in their computation. Therefore, these data are not adequate to use in the GPD+ validation. However, the analysis of the root mean square (RMS) value of the WTC differences, function of distance from coast, can be valuable to inspect the correction in coastal regions, where the methodology is committed to ameliorate the WTC. For this assessment, GNSS-derived WTC have been computed at a network of 60 GNSS stations using the methodology explained in Vieira et al. (2019b). This network has a good geographical distribution and covers regions around the world with different atmospheric variability conditions. This data set consists of WTC measurements at each station location for the whole period of observations available for that station, allowing a non-collocated comparison with WTC estimations at MWR points. Differences between these GNSS-derived WTC and the on-board MWR and the GPD+ WTC retrievals, respectively, have been computed and analysed for the whole Envisat mission. Only GPD+ estimates retrieved using observations are selected. For the acquisition instant of each MWR-derived WTC, a GNSS-derived WTC is computed, at the station location, for the same instant using interpolation in time; at the same acquisition epoch and location, the GPD+ WTC is also available, being the latter collocated both in time and space with each other and over ocean. For each pair of WTCs (MWR and GNSS-derived WTCs and GPD+ and GNSS-derived WTCs, relative to the same instant), the distance from coast of each altimeter point is computed. This process is repeated for each GNSS station with surrounded altimetry measurements and then the whole set of stations is considered, in order to obtain representative results for the whole globe. Differences are binned into 5-km intervals and the RMS values computed function of distance from coast. The results are shown in Fig. 7, for distances up to 65 km from the coast, where red and grey bars represent the number of measurements used to compute the RMS of the differences GNSS-MWR and GNSS-GPD, respectively. The number of differences is not the same in each case. While in the second case only GPD+ WTC retrieved from the observations have been selected (those estimated from the model where discarded), in the first case only valid MWR values and those rejected solely based on the criteria of distance from coast were kept (otherwise the invalid measurements would overestimate the results). As expected, the number of GNSS-MWR differences is generally smaller than the number of GNSS-GPD+ differences. Figure 7 therefore shows that the GPD+ methodology recovers the WTC not only along the coastal areas, but also offshore.

The increase in the RMS value of the GNSS-MWR differences in the closest 25 km of the coast, seen in Fig. 7, is a clear indicator of the loss of accuracy of MWR-derived WTCs in this coastal strip. This also shows that when all rejection criteria except the one concerned with the distance from coast are applied, land contamination is still present, and that this criterion is necessary. The decrease in the number of GNSS-MWR differences indicates, in turn, the existence of invalid MWR-derived WTC, not used in these statistics. On the contrary, the RMS of the differences GNSS-GPD+ decreases when approaching

https://doi.org/10.5194/essd-2019-171
Preprint. Discussion started: 17 October 2019

coast. Generally, the stations and the number of differences increase, indicating that the GPD+ WTCs estimates are valid up to the coastline and that these WTC values are recovered at all along-track points without valid MWR-derived WTCs.

3.2 Accuracy assessment of the Envisat GPD+ WTC

Water vapour content can be accurately obtained by radio sounding data that could ideally be employed to validate the GPD+ estimates. Despite having high vertical resolution, radiosonde measurements are distributed only over limited areas, i.e., regions where stations are located, do not cover oceanic regions and are very scarce over the Southern Hemisphere (Ye et al., 2017). Therefore, their low temporal and spatial resolutions have reduced their use as a validation tool in the context of satellite altimetry.

For this reason, the GPD+ products have been validated through various SLA variance statistical analyses, assessing simultaneously the impact of the correction on sea level variability. The reasoning for adopting this analysis is that the larger the variance reduction in the SLA signal when using a certain WTC, the better is the correction, i.e., the larger is the reduction in the SLA error, and closer to a pure oceanic signal is the SLA dataset that uses that correction. Therefore, three SLA datasets of collocated along-track points were derived using the same standard corrections (Sect. 1) but the WTC, which can be the Composite correction present in AVISO CorSSH L2P products (Comp), the GPD+ or the ERA Interim WTCs. Differences between each pair of SLA data sets are computed along track and at crossovers and the weighted variance estimated for the period spanning the whole Envisat period, with latitude-dependent weights. For the computation of the crossovers, only measurements with a temporal difference less than 10 days were used. Besides the temporal analysis, the variance differences are also mapped globally for the analysis of their spatial distribution. In this latter case, the variances of the SLA differences are gridded onto 4-degree spatial resolution cells. Along-track SLA variance differences are also computed as function of latitude and distance from coast, where the variance for the whole Envisat period is computed over bins of latitude and distance from coast. Figure 8 illustrates the obtained results for the period of the whole Envisat mission. From this figure, it is observed that the GPD+ WTC for Envisat represents a significant improvement when compared to the other WTC selected for this validation. In these comparisons, all points with valid SLA have been selected. For those points with the Composite WTC outside limits or absent, the ERA Interim WTC value has been assumed for this correction. Using the GPD+ WTC instead of the Comp WTC (Fig.8a) leads to an improvement in the variance of the oceanic signal of 0.5 cm^2 in average, this improvement increasing in the second half of the period, where values of 2 cm^2 can be reached in some cycles. Adopting the GPD+ WTC instead of the ERA Interim model one (Fig. 8b) leads to a reduction in SLA variance which, in average, is in the range of 1 and 2 cm^2. For both comparisons, the SLA reduction is more noticeable in the along-track analysis than in the crossover analysis. Usually the SLA variance reduction is analysed at crossover locations, however since oceanic variability with periods lower than 10 days is neglected when doing this analysis, whilst preserved in the along-track differences, both diagnostics are considered complementary.

Figure 9 shows the reduction in SLA variance globally, after being spatially averaged, estimated at crossovers for the differences GPD+ and Comp WTCs, and GPD+ and ERA WTCs, on top and bottom plots, respectively. In these plots, blueish

https://doi.org/10.5194/essd-2019-171
Preprint. Discussion started: 17 October 2019

colours represent an improvement in the SLA dataset by reducing the SLA variance. The improvement of the GPD+ WTC over the model WTC (Fig. 9b) is clear with maximum values of variance reduction in the tropical oceans, particularly over the Pacific Ocean. The improvement over the Southern Ocean and around the coast of Antarctica shows that the model WTC is not able to capture the full variability of the WPD field yet. Regarding the comparison with the Comp WTC (Fig. 9a), although the SLA improvement when using GPD+ WTC is smaller than the previous one, it can be emphasized that the improvement is global, therefore not limited to the coastal regions. Therefore, the use of third-party data can help the description of the WPD field.

SLA variance differences have also been analysed as function of latitude and distance from coast and the results are shown in Fig. 10. Both the differences between GPD+ and ERA WTCs or GPD+ and Comp WTCs are represented. The variance of the SLA dataset is reduced when GPD+ is used instead of the other WTCs for all latitudes (Fig. 10a). The improvement of the GPD+ WTC with respect to the model one is maximum over latitudes where maximum atmospheric water content can be found, namely over the subtropical ocean and over latitudes where the western-boundary currents flow, particularly in the northern hemisphere where the variance reduction surpluses 2 cm^2. As expected, the improvement is smaller for the comparison with the Comp WTC. Leading to an improvement in the SLA variance of 0.4 cm^2 in average, the GPD+ WTC has its best performance against the Comp WTC in the extratropical ocean, especially in the northern one. The increase in the reduction of the SLA variance at these latitudes is associated to a better description of the WPD field in the coastal regions northwards of the regions where the western boundary currents flow (off Newfoundland and in the Sea of Okhotsk), as can be concluded from the maps showing the reduction in SLA variance for the difference GPD+ and Comp WTCs, computed along-track and spatially averaged at each 4-degree cell (not shown). The SLA dataset is also improved over the coastal regions when the GPD+ WTC is applied (Fig. 10b). The improvement over the Comp WTC is larger in the nearest 50 km to the coast, where the reduction in variance varies is, in average, 0.8 cm^2. As the distance to shore increases, the reduction in variance decreases, although still negative and around -0.5 cm^2, since the number of invalid MWR-derived WTCs decrease offshore and so does the number of Comp estimates. On the opposite, the improvement over the model correction increases with distance from coast due to the improvement in the description of the WPD field over open ocean (cf. Fig. 9). The improvement obtained with the GPD+ methodology in the coastal areas due to the increase in the number of points with valid SLA value is unfortunately not completely evident in these depicted results, since part of the points that do not possess a valid MWR-derived correction, for which a GPD+ estimate is computed, are discarded from the analysis.

4 Data Availability

The GPD+ WTCs are freely available in NetCDF format at the UPorto's Satellite Altimetry repository https://doi.org/10.23831/FCUP_UPORTO_GPDPlus_v1.0 (Fernandes et al., 2019) and at the AVISO (Archiving, Validation and Interpretation of Satellite Oceanographic data) webpage (https://www.aviso.altimetry.fr/en/data/products/auxiliary-products/gpd-wet-tropospheric-correction.html).

https://doi.org/10.5194/essd-2019-171
Preprint. Discussion started: 17 October 2019

5 Conclusions

The wet tropospheric correction (WTC) is still considered an important source of error in satellite altimetry, particularly in coastal and polar regions, where the retrieval of the wet path delays from the microwave radiometer (MWR) measurements on board the altimetry missions leads to invalid values. During the data processing aiming at deriving the sea level anomaly, altimeter measurements are discarded if the WTC is absent, which is frequent in coastal and polar regions. In the last years, a huge effort has been made to develop methodologies capable of computing WTC estimates where the correction is absent, while keeping the high-accuracy of MWR-derived WTC values. A few methodologies emerged, among which the GPD and its most-updated version GPD+ have proven to be the most effective in reducing the SLA variability due to non-ocean phenomena, simultaneously leading to the recovery of a significant number of measurements.

This paper describes the GPD+ WTC database and exemplifies the results using as input the Envisat FRM V3.0. The GPD+ WTC equals the MWR-derived WTC whenever this latter is valid, thus preserving its accuracy. For those MWR-derived WTCs detected by the algorithm as invalid, a new estimate and its associated mapping error are computed. The GPD+ algorithm has been trained to detect land, ice and outlier-contaminated measurements besides those identified in the GDR data already. On top of preserving the accuracy of the WTC derived from the on-board MWR measurements, the GPD+ algorithm guarantees the continuity and consistency of the output WTC globally.

Prior studies using a previous GPD+ version (e.g., GPD algorithm cf. Fernandes et al. (2015)) show that the GPD WTC led to a significant improvement of the SLA dataset for T/P and ESA-funded missions, since these, particularly the latter, had an on-board MWR which retrieval algorithms were unable to deal with coastal- and ice-contaminated measurements. For these missions, the GPD WTC was proven to be the preferred WTC to be used in the definition of the SLA field, when compared to the baseline MWR one, the model-derived one and the AVISO reference composite correction, provided in their products. The main advantage of the methodology when applied to the T/P mission is that it corrects the interpolation anomalies present in the second part of the mission, particularly noticeable in the Indian Ocean, which would otherwise seriously affect the calculation of the mean sea level at regional scales (Fernandes et al., 2015). The GPD+ WTCs for GFO and CryoSat-2 missions have been described in Fernandes and Lázaro (2016). Despite the MWR on board GFO mission being considered a stable and accurate instrument, it had periods of malfunctioning, particularly in the last years of the mission. In addition to improving the derived SLA dataset, by reducing the error associated with non-pure oceanic signal, the GPD+ recovers the WTC for the periods during which the GFO MWR was defective. For CryoSat-2 mission, without an on-board MWR and therefore without a WTC relying on observations, the GPD+ is computed for all along-track points. GPD+ WTC thus replaces the NWM-derived WTC that otherwise would have to be used instead. For this mission, the exploitation of third-party data has been proven to be very effective. As the results in this paper show, the NWM-derived WTCs are still inaccurate since they are limited to a poor spatial and temporal resolution. Products available for Jason missions already possess a coastally improved WTC (Brown, 2010). Still, although small, some improvement, particularly at high latitudes and mainly for Jason-1 can be achieved when the GPD+ correction is used in the generation of the SLA dataset (Fernandes et al., 2015).

https://doi.org/10.5194/essd-2019-171
Preprint. Discussion started: 17 October 2019

Many authors have also proven the positive impact of the GPD+ corrections, particularly in coastal studies, e.g. Handoko et al. (2017) in the Indonesia region and Dinardo et al. (2018) in the German Bight.

Taken as a whole, the GPD+ algorithm possesses the advantage of being able to compute the WTC at a considerable number of along-track points with an invalid/inexistent MWR-derived WTC, therefore leading to the recovery of the SLA signal at these points. Moreover, the GPD+ WTC is a continuous correction in the ocean/land interface region, as well as in the polar regions. The scientific novelty and practical significance for the common satellite altimetry user is that the GPD-corrected SLA dataset can be used for coastal applications, constituting a major step forward for satellite altimetry to become a tool for coastal management.

Despite significant efforts in the past to improve the WPD calculation at GNSS-station height and the sea-level reduction of the correction to use in satellite altimetry over ocean, the unpredictable way the WPD varies with altitude is still a factor constraining the precise GNSS data reduction procedure, since all other data are provided at sea level. Therefore, despite the modelling of the 4D variability of the WPD field being still under research (Vieira et al., 2019c), it is expected that the GPD+ continues to be the WTC most effective in reducing the sea level variance due to non-oceanic signals, since the whole GNSS data processing upstream to the GPD+ computation is also performed at UPorto.

Upcoming developments include: i) the inclusion of an ameliorate modelling of the WTC vertical variability (Vieira et al., 2019c), leading to a better consistency of the various datasets combined in the OA procedure; ii) the extension of the corrections to all surface types with new estimates over all regions where observations exist, e.g. large lakes and rivers where valid MWR and GNSS can be exploited; iii) and, for the older missions, the replacement of the ERA Interim model by ERA5, the most recent reanalysis by ECMWF (Vieira et al., 2019d).

Author Contributions.

MJF and CL developed the methodology and the code. All authors performed the simulations. CL prepared the manuscript with contributions from all co-authors. All authors have read and approved the final paper.

Competing Interests.

The authors declare that they have no conflict of interest.

Acknowledgements.

The results here provided for Envisat FRM V3.0 were obtained in the scope of the ESA funded project CLS-SCO-17-0034, ENVISAT RA-2 LEVEL 1B ESL AND PROTOTYPE MAINTENANCE SUPPORT, Subcontract to ESA/Contract N° 4000110859/14/I-AM. The authors thank Radar Altimeter Database System (RADS) for providing the GPD+ input altimeter

https://doi.org/10.5194/essd-2019-171
Preprint. Discussion started: 17 October 2019

Open Access Earth System Science Data Discussions

data for all missions except Envisat, Aviso+ (https://www.aviso.altimetry.fr/), as part of the Ssalto ground processing segment, for the production and distribution of CorSSH L2P altimeter products, the European Centre for Medium-Range Weather Forecasts (ECMWF) for making both the ECMWF operational and the ERA Interim models available, and all institutions providing the water vapour products used in this study: National Oceanic and Atmospheric Administration (NOAA) – Comprehensive Large Array-Data Stewardship System (CLASS) and Remote Sensing Systems. SSM/I and SSMIS data are produced by Remote Sensing Systems and sponsored by the NASA Earth Science MEaSUREs Program and are available at www.remss.com.

Financial Support.

Telmo Vieira is supported by the Fundação para a Ciência e a Tecnologia (FCT) through the PhD grant SFRH/BD/135671/2018, funded by the European Social Fund and by Ministério da Ciência, Tecnologia e Ensino Superior (MCTES). This research was also supported by Centro Interdisciplinar de Investigação Marinha e Ambiental (CIIMAR) through the project with reference UID/Multi/04423/2019.

References

Askne, J. and Nordius, H.: Estimation of Tropospheric Delay for Microwaves From Surface Weather Data, Radio Sci., 22(3), 379–386, doi: 10.1029/RS022i003p00379, 1987.

AVISO: Along-track Level-2+ (L2P) SLA Product Handbook, SALP-MU-P-EA-23150-CLS, 1 rev 0, 2017.

Bosser, P. Bock, O., Pelon, J., Thom, C.: An improved mean-gravity model for GPS hydrostatic delay calibration, IEEE Geosci. Rem. Sens. Letters, 4(1), 3–7, doi: 10.1109/LGRS.2006.881725, 2007.

Bretherton, F P., Davis, R. E. and Fandry, C. B.: A technique for objective analysis and design of oceanographic experiment applied to MODE-73, Deep-Sea Res., 23, 559–582, doi: 10.1016/0011-7471(76)90001-2, 1976.

Brown, S.: A novel near-land radiometer wet path-delay retrieval algorithm: Application to the Jason-2/OSTM advanced microwave radiometer, IEEE Trans. Geosci. Remote Sens., 48, 1986–1992, doi: 10.1109/TGRS.2009.2037220, 2010.

Chelton, D. B., Ries, J. C., Haines, B. J., Fu, L. L., Callahan, P. S.: Satellite Altimetry. In Satellite Altimetry and Earth Sciences: A Handbook of Techniques and Applications; Fu, L.L., Cazenave, A., Eds.; Academic: San Diego, CA, USA; Volume 69, 1–131, 2001.

Cipollini, P., Benveniste, J., Birol, F., Fernandes, M. J., Obligis, E., Passaro, M., Strub, P. T., Valladeau, G., Vignudelli, S., Wilkin J.: Satellite altimetry in coastal regions. In D. Stammer and A. Cazenave, (Eds.), Satellite Altimetry Over Oceans and Land Surfaces, 343–380, CRC Press. ISBN: 9781498743457, 2017.

https://doi.org/10.5194/essd-2019-171
Preprint. Discussion started: 17 October 2019

Dinardo, S., Fenoglio-Marc, L., Buchhaupt, C., Becker, M., Scharroo, R., Fernandes, M. J., Benveniste, J.: Coastal SAR and PLRM altimetry in German Bight and West Baltic Sea. Advances in Space Research, 62(6), 1371-1404. doi:10.1016/j.asr.2017.12.018, 2018.

Dousa, J. and Elias, M.: An improved model for calculating tropospheric wet delay, Geophys. Res. Lett., 41, 4389–4397, doi:10.1002/2014GL060271, 2014.

European Space Agency (ESA) (2018), RA2 Products and Algorithms, webpage https://earth.esa.int/web/sppa/mission-performance/esa-missions/envisat/ra2/products-and-algorithms/products-information, accessed July 2019.

European Space Agency (ESA) (2019), Envisat Altimetry Full Mission Reprocessing V3.0, webpage https://earth.esa.int/web/guest/content/-/article/envisat-altimetry-v3-0-full-mission-reprocessing, accessed July 2019.

Fernandes, M. J., Lázaro, C.: GPD+ Wet Tropospheric Corrections for CryoSat-2 and GFO Altimetry Missions, Remote Sens. 2016, 8(10), 851, doi: 10.3390/rs8100851, 2016.

Fernandes, M. J., Lázaro, C.: Independent assessment of Sentinel-3A wet tropospheric correction over the open and coastal ocean, Remote Sens., 10(3), 484. doi:10.3390/rs10030484, 2018.

Fernandes, M. J., Lázaro, C., Ablain, M., Pires, N.: Improved wet path delays for all ESA and reference altimetric missions, Remote Sens. Environ., 169, 50–74, doi: 10.1016/j.rse.2015.07.023, 2015.

Fernandes, M. J., Lázaro, C., Nunes, A. N., Scharroo, R.: Atmospheric Corrections for Altimetry Studies over Inland Water, Remote Sens., 6(6), 4952-4997. doi:10.3390/rs6064952, 2014.

Fernandes, M. J., Lázaro, C., Vieira, E., Vieira, T.: UPorto GPD+ Wet Tropospheric Correction. Dataset available at: https://doi.org/10.23831/FCUP_UPORTO_GPDPlus_v1.0 (last access: 16 September 2019), 2019.

Fernandes, M. J., Nunes, A. N., and Lázaro, C.: Analysis and Inter-Calibration of Wet Path Delay Datasets to Compute the Wet Tropospheric Correction for CryoSat-2 over Ocean, Remote Sens., 5(10), 4977-5005. doi:10.3390/rs5104977, 2013b.

Fernandes, M. J., Pires, N., Lázaro, C., Nunes, A. L.: Tropospheric delays from GNSS for application in coastal altimetry, Adv. Space Res., 51(8), 1352–1368, doi: 10.1016/j.asr.2012.04.025, 2013a.

Fernandes, M. J., Barbosa, S., Lázaro, C.: Impact of Altimeter Data Processing on Sea Level Studies. Sensors, 6(3), 131-163. doi:10.3390/s6030131, 2006.

Handoko, E., Fernandes, M. J., Lázaro, C.: Assessment of Altimetric Range and Geophysical Corrections and Mean Sea Surface Models—Impacts on Sea Level Variability around the Indonesian Seas. Remote Sens., 9(2), 102. doi:10.3390/rs9020102, 2017.

https://doi.org/10.5194/essd-2019-171
Preprint. Discussion started: 17 October 2019

Kouba, J.: Implementation and testing of the gridded vienna mapping function 1 (VMF1), J. Geod., 82, doi: 10.1007/s00190-007-0170-0, 193–205, 2008.

Legeais, J.-F., Ablain, M., Zawadzki, L., Zuo, H., Johannessen, J. A., Scharffenberg, M. G., Fenoglio-Marc, L., Fernandes, M. J., Andersen, O. B., Rudenko, S., Cipollini, P., Quartly, G. D., Passaro, M., Cazenave, A., and Benveniste, J.: An improved and homogeneous altimeter sea level record from the ESA Climate Change Initiative, Earth Syst. Sci. Data, 10, 281–301, https://doi.org/10.5194/essd-10-281-2018, 2018.

Mercier, F.: Amélioration de la correction de troposphère humide en zone côtière. Rapport Gocina, CLS-DOS-NT-04-086, 2003.

Mercier, F., Rosmorduc, V., Carrere, L., Thibaut, P.: Coastal and Hydrology Altimetry Product (PISTACH) Handbook, CLS-DOS-NT-10-246, Issue 1.0, CNES, 2010.

Pany, T., Pesec, P. and Stangl, G.: Atmospheric GPS slant path delays and ray tracing through numerical weather models, a comparison, Phys. Chem. Earth PT A, 26(3), 183–188, doi: 10.1016/S1464-1895(01)00044-8, 2001.

Quartly, G. D., Legeais, J., Ablain, M., Zawadzki, L., Fernandes, M. J., Rudenko, S., Carrère, L., García, P. N., Cipollini, P., Andersen, O. B., Poisson, J. C., Mbajon Njiche, S., Cazenave, A., Benveniste, J.: A new phase in the production of quality-controlled sea level data. Earth Syst. Sci Data, 9(2), 557-572. doi:10.5194/essd-9-557-2017, 2017.

Scharroo, R., Leuliette, E. W., Lillibridge, J. L., Byrne, D., Naeije, M. C., Mitchum, G. T.: RADS: Consistent multi-mission products, Proceedings of the 20 Years of Progress in Radar Altimetry Symposium, Venice, Italy, 20–28 September 2012.

Steunou, N., Picot, N., Sengenes, P., Noubel, J., Frery, M.L.: AltiKa Radiometer: Instrument Description and In–Flight Performance, Mar. Geod., 38:sup1, 43–61, DOI: 10.1080/01490419.2015.1006381, 2015.

Stum, J., Sicard, P., Carrere, L. Lambin, J.: Using Objective Analysis of Scanning Radiometer Measurements to Compute the Water Vapor Path Delay for Altimetry, IEEE Trans. Geosci. Remote Sens., 49, 9, 3211–3224, doi: 10.1109/TGRS.2011.2104967, 2011.

Vieira, E., Lázaro, C., Fernandes, M. J.: Spatio-temporal variability of the wet component of the troposphere – Application to Satellite Altimetry, Advances in Space Research, 63(5), 1737-1753. doi: 10.1016/j.asr.2018.11.015, 2019a.

Vieira, T., Fernandes, M. J., Lázaro, C.: Independent Assessment of On-Board Microwave Radiometer Measurements in Coastal Zones Using Tropospheric Delays from GNSS, IEEE Trans. Geosci. Remote Sens., 57, 1804–1816, doi: 10.1109/TGRS.2018.2869258, 2019b.

Vieira, T., Fernandes, M. J., Lázaro, C.: Modelling the altitude dependence of the Wet Path Delay for coastal altimetry using 3-D parameters from ERA5. Remote Sens. To be submitted, 2019c.

https://doi.org/10.5194/essd-2019-171
Preprint. Discussion started: 17 October 2019

Vieira, T., Fernandes, M. J., Lázaro, C.: Impact of the new ERA5 Reanalysis in the Computation of Radar Altimeter Wet Path Delays. IEEE Trans. Geosci. Remote Sens. doi: 10.1109/TGRS.2019.2929737, 2019d.

595 Vignudelli, S., Cipollini, P., Gommenginger, C., Snaith, H. M., Coelho, E., Fernandes, J., Gomez-Henri, J., Martin-Puig, C., Woodworth, P. L., Dinardo, S., Benveniste, J. J.: The COASTALT Project: Towards an Operational Use of Satellite Altimetry in the Coastal Zone, American Geophysical Union, Fall Meeting 2009, abstract id. OS22A-02, 2009.

Ye, S., Xia, P., and Cai, C.: Optimization of GPS water vapor tomography technique with radiosonde and COSMIC historical data, Ann. Geophys., 34, 789–799, doi:10.5194/angeo-34-789-2016, 2016.

600

Table 1. Total Column Water Vapour (TCWV) availability (Fernandes et al., 2016).

Satellite/Sensor	Availability
DMSP-F10/SSM/I	December 1990–November 1997
DMSP-F11/SSM/I	November 1991–May 2000
DMSP-F13/SSM/I	March 1995–November 2009
DMSP-F14/SSM/I	May 1997–August 2008
DMSP-F16/SSM/IS	since October 2003
DMSP-F17/SSM/IS	since December 2006
NOAA-15/AMSU-A	since July 2003
NOAA-16/AMSU-A	July 2003–June 2014
NOAA-17/AMSU-A	July 2003–April 2013
NOAA-18/AMSU-A	since August 2005
NOAA-19/AMSU-A	since May 2009
MetOp-A/AMSU-A	since May 2007
MetOp-B/AMSU-A	since April 2013
AQUA/AMSR-E	May 2002–October 2011
GCOM-W1/AMSR-2	since May 2012
TRMM/TMI	December 1997–March 2015
Coriolis/WindSat	since February 2003

https://doi.org/10.5194/essd-2019-171
Preprint. Discussion started: 17 October 2019

Table 2. Data content in each GPD+ WTC NetCDF file, for the time and location of each altimetry mission measurement (Fernandes et al., 2019).

Variable	Description
time_01	time of measurement, UTC seconds since 2000-01-01 00:00:00.0
lat_01	latitude of measurement, as in the GDR file
lon_01	longitude of measurement, as in the GDR file
GPD_wet_tropo_cor _01	GPD+ wet tropospheric correction (metres)
GPD_wet_tropo_cor_qual_01	validity flag of the GPD+ estimate: 0-valid, 1-invalid

Table 3. Mission Code used in the name of the GPD+ Datasets (Fernandes et al., 2019) and their availability.

Mission Code	Mission	Start Time	End Period
TP	TOPEX/Poseidon	1992/07 (cycle 1)	2005/08 (cycle 481)
J1	Jason-1	2002/01 (cycle 1)	2012/03 (cycle 374*)
J2	OSTM/Jason-2	2008/05 (cycle 1)	2018/06 (cycle 353)
J3	Jason-3	2016/02 (cycle 1)	2018/05 (cycle 084)
E1	ERS-1	1991/08 (phase A, cycle 1)	1996/04 to phase g, cycles 156* or 53**
E2	ERS-2	1995/04 (cycle 1)	2011/05 (cycle 167)
EN	Envisat	2002/04 (cycle 1)	2012/03 (cycle 113)
GFO	GEOSAT Follow-On	2000/01 (cycle 37)	2008/09 (cycle 223)
C2	CryoSat-2	2010/07 (sub-cycle 4)	2018/06/30 (sub-cycle 106)
SA	SARAL/AltiKa	2013/03 (cycle 1)	2016/01 (cycle 30)

* RADS convention

** AVISO convention

https://doi.org/10.5194/essd-2019-171
Preprint. Discussion started: 17 October 2019

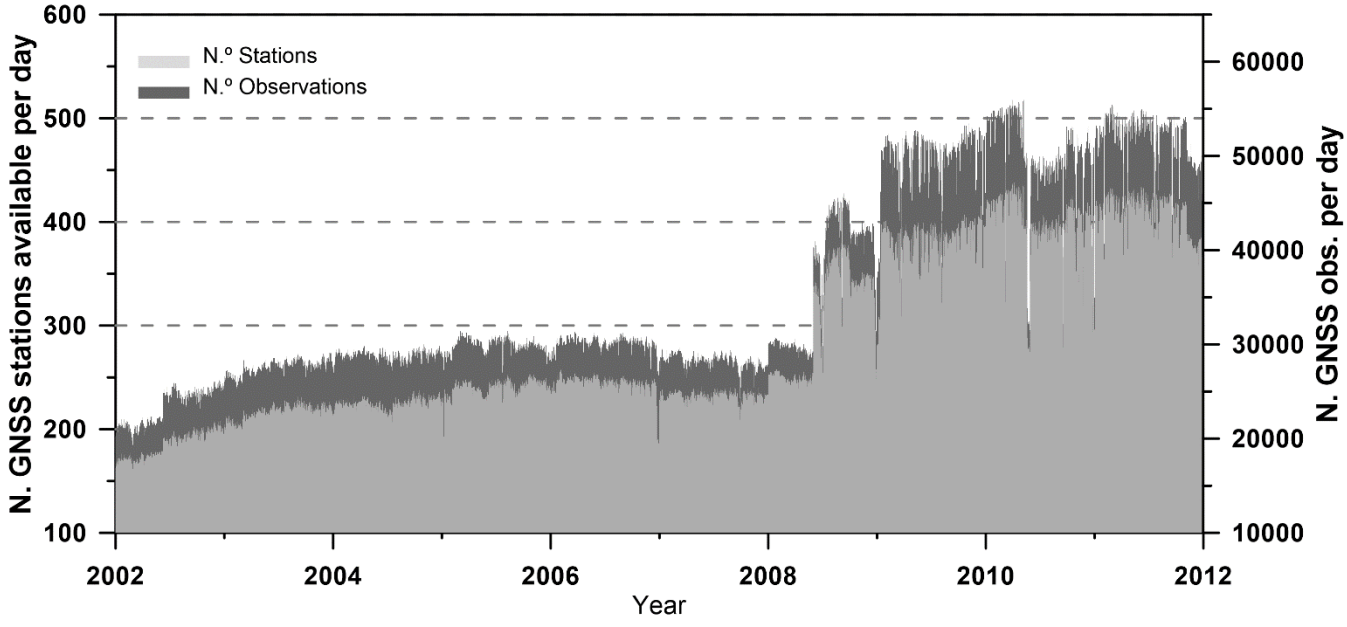

Figure 1 Number of GNSS stations used in the GPD+ over time (light grey) and number of available GNSS observations per day (dark grey), for the Envisat period. All GNSS stations are at a distance from coast less than 100 km.

https://doi.org/10.5194/essd-2019-171
Preprint. Discussion started: 17 October 2019

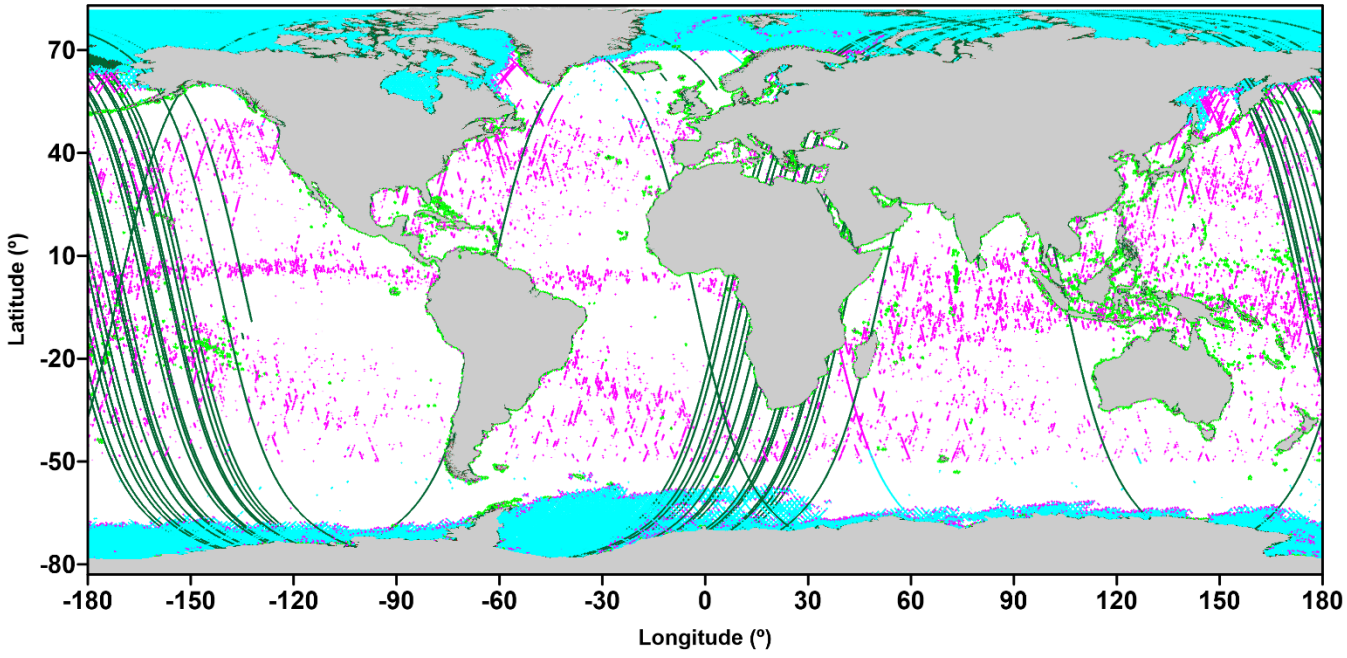

635

Figure 2 Invalid MWR-derived WTC for Envisat cycle 12: correction contaminated due to ice, correction contaminated due to rain and outliers; points flagged as coastal, may possess a correction contaminated by land; no available MWR-derived WTC value (the "fill value" is given). A note must be made that there are several points with available MWR-derived field but with an invalid value and without any error flag, that are detected and flagged by the GPD+ algorithm.

https://doi.org/10.5194/essd-2019-171
Preprint. Discussion started: 17 October 2019

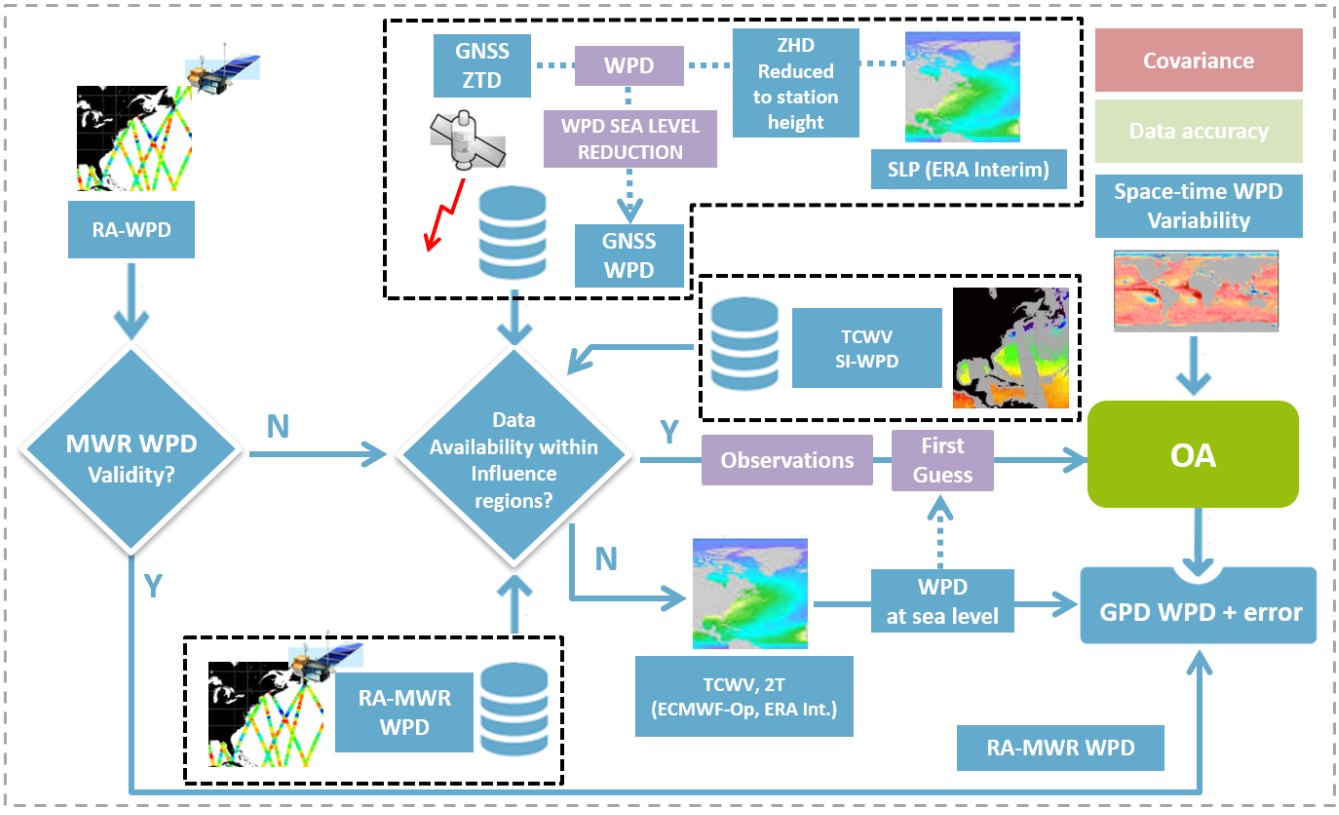

Figure 3 Fluxogram of the GPD+ algorithm.

https://doi.org/10.5194/essd-2019-171
Preprint. Discussion started: 17 October 2019

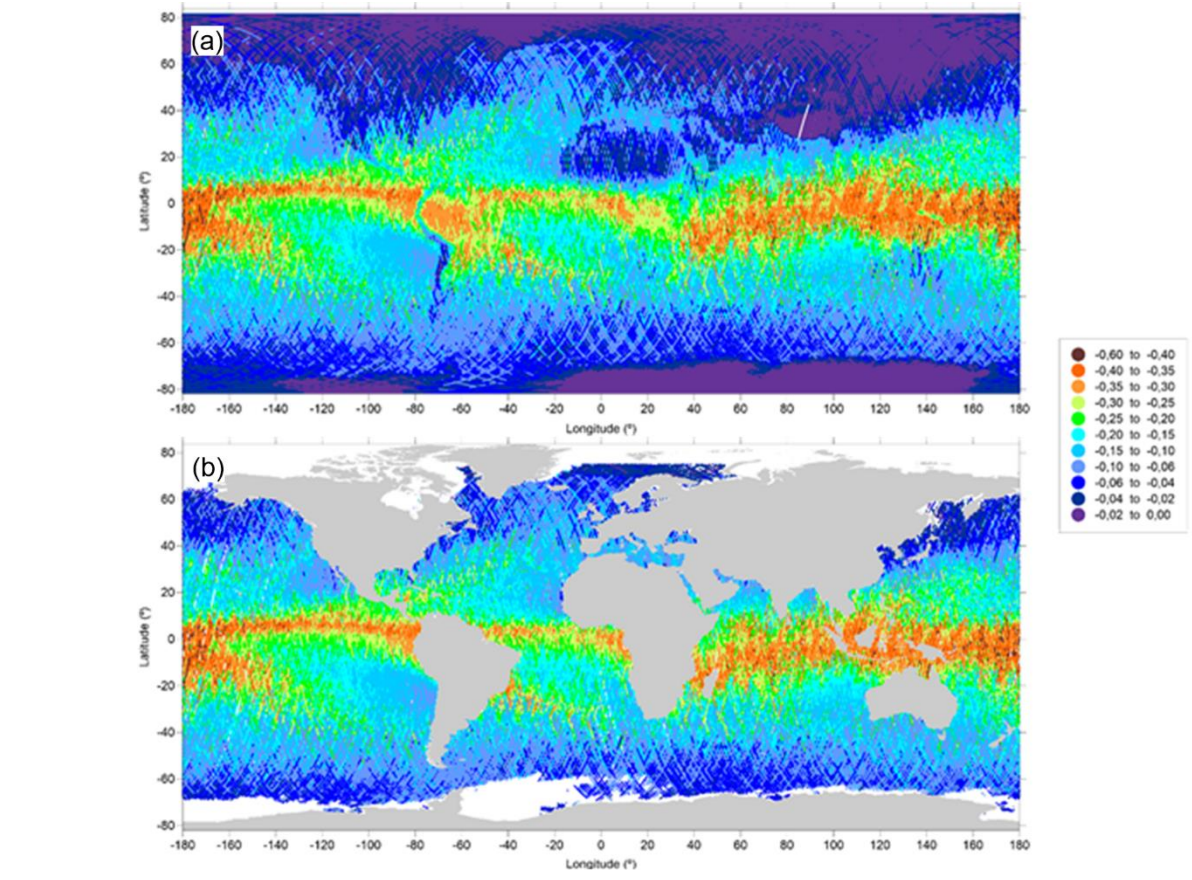

Figure 4 GPD+ WTC, in metres, for Envisat cycle 012: (a) global coverage and (b) correction over oceanic regions with valid SLA.

https://doi.org/10.5194/essd-2019-171
Preprint. Discussion started: 17 October 2019

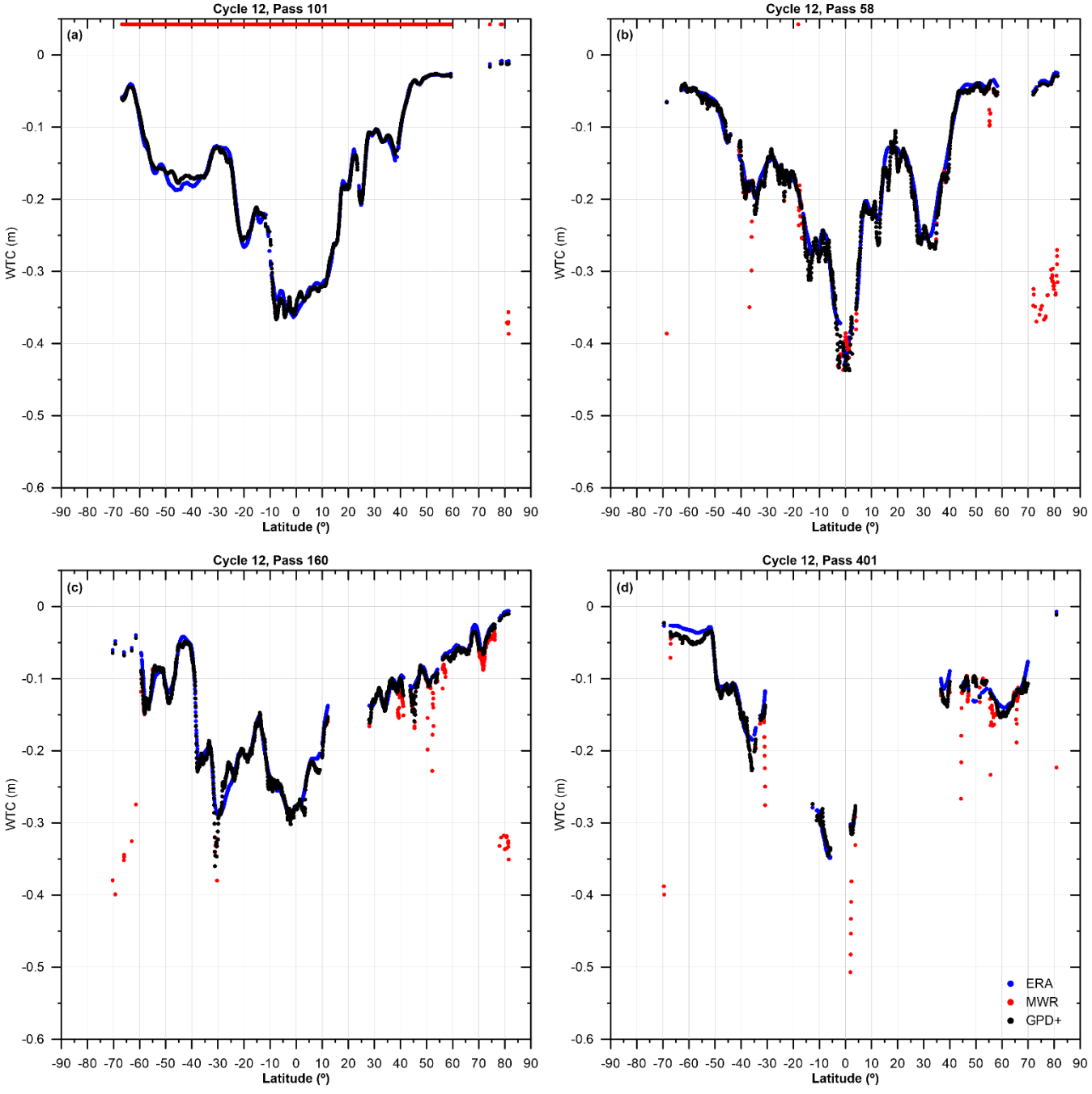

Figure 5 GPD+ WTC (black) for some Envisat tracks, exemplifying several issues commonly encountered in the on-board MWR-derived WTC (red) that no longer exist in the GPD+ WTC (a) unavailability of the correction (Cycle 12, pass 101); (b) correction contaminated by ice (Cycle 12, pass 58); (c): existence of outliers (Cycle 12, pass 160); (d) correction contaminated by land proximity (Cycle 12, Pass 401). In the top-left plot it is possible to see the improvement in the description of the WTC signal in terms of small

https://doi.org/10.5194/essd-2019-171
Preprint. Discussion started: 17 October 2019

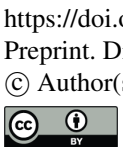

spatial scales when compared to the ERA Interim WTC (in blue). In these plots, the corrections are shown only for points with valid SLA values.

675

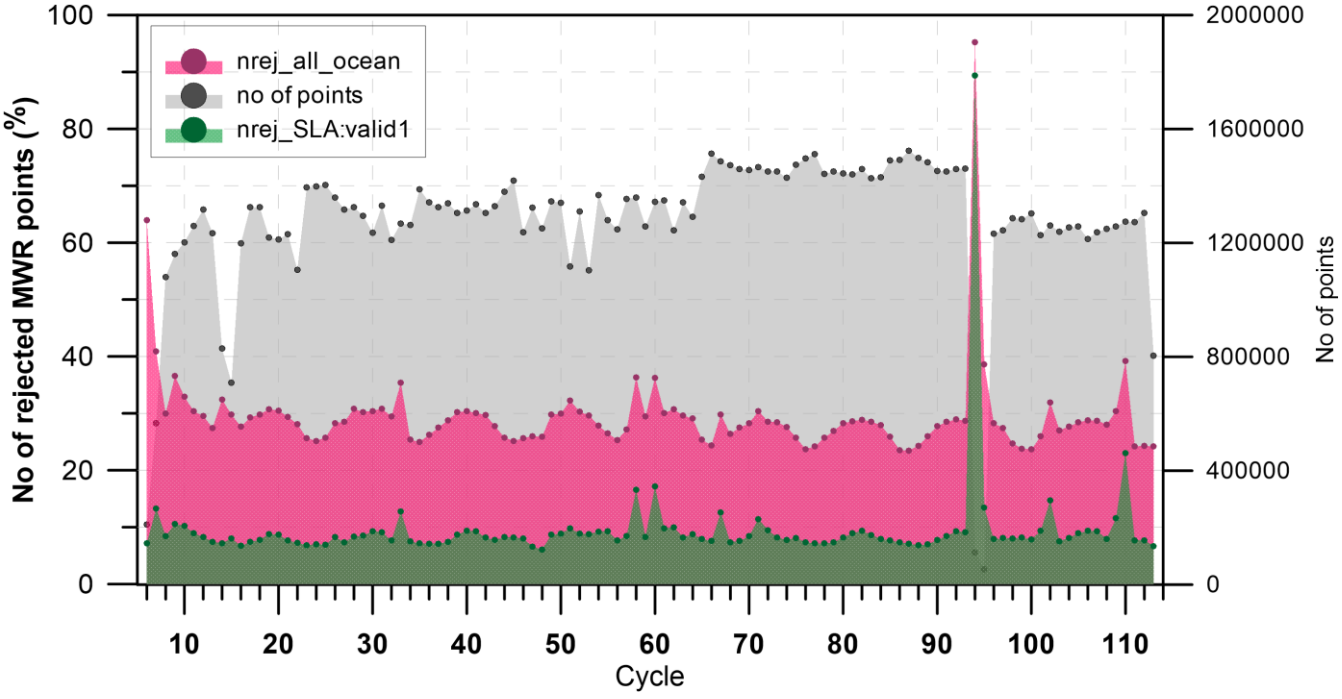

Figure 6 Summary, for the whole Envisat period, of the percentage of points: (pink) with a rejected MWR-derived WTC, for which a GPD+ estimate has been computed; (green) for which a valid SLA value could be computed after the estimation of the WTC by the GPD+. Also shown in grey is the number of points with valid SLA values per cycle.

https://doi.org/10.5194/essd-2019-171
Preprint. Discussion started: 17 October 2019

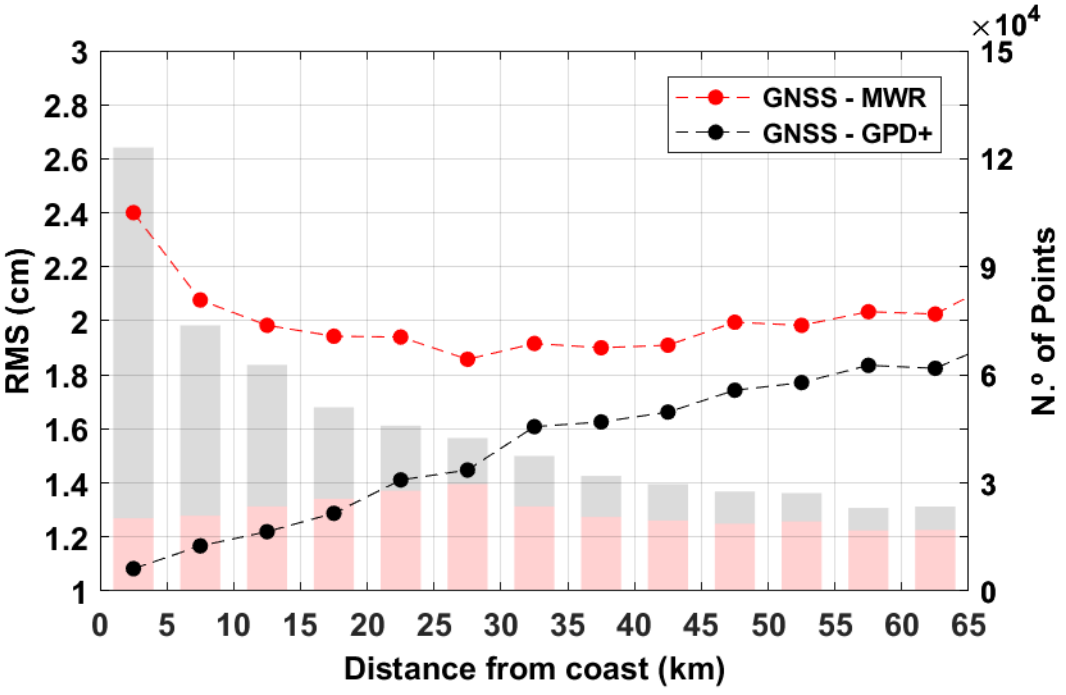

680

Figure 7 RMS of WTC differences (left axis) and number of altimetry measurements used (right axis) for the Envisat mission, function of distance from coast. Red bars represent the number of measurements used to compute the RMS of the differences GNSS-MWR, while grey bars represent the number of points used to compute the RMS of the differences GNSS-GPD+. In the comparison GNSS – MWR only valid MWR-derived observations have been used.

https://doi.org/10.5194/essd-2019-171
Preprint. Discussion started: 17 October 2019

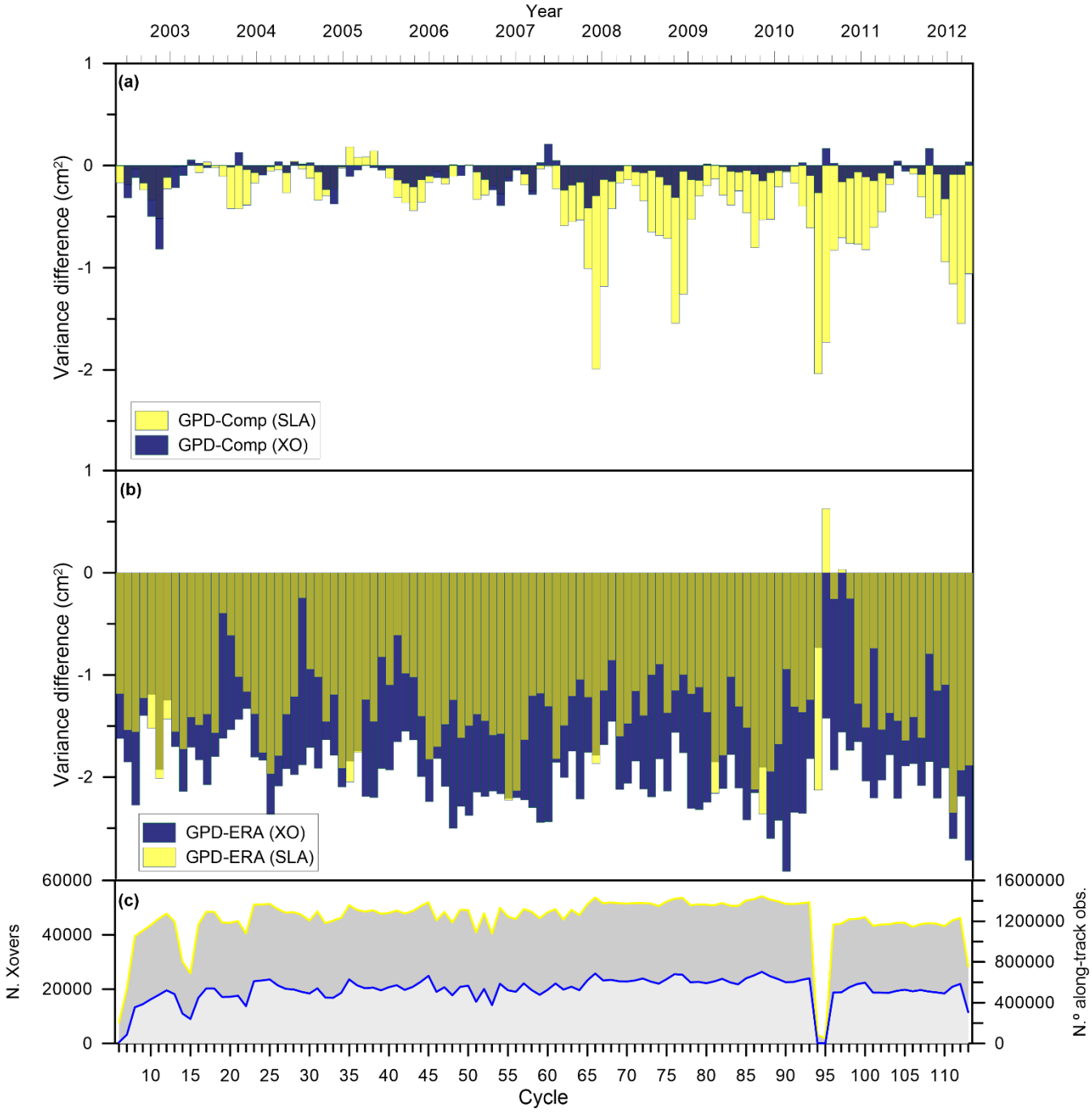

Figure 8 Temporal evolution of weighted SLA variance differences (cm^2) along track (yellow) and at crossovers (blue) between (a) GPD+ and the Composite WTCs and (b) between GPD+ and ERA Interim WTCs. Bottom plot (c) shows the number of crossovers ("N. Xovers", blue) and the number of along-track (yellow) pairs used, per cycle, in the analyses. To facilitate the analysis, both cycle number (bottom x-axis) and time (year, top x-axis) are used.

https://doi.org/10.5194/essd-2019-171
Preprint. Discussion started: 17 October 2019

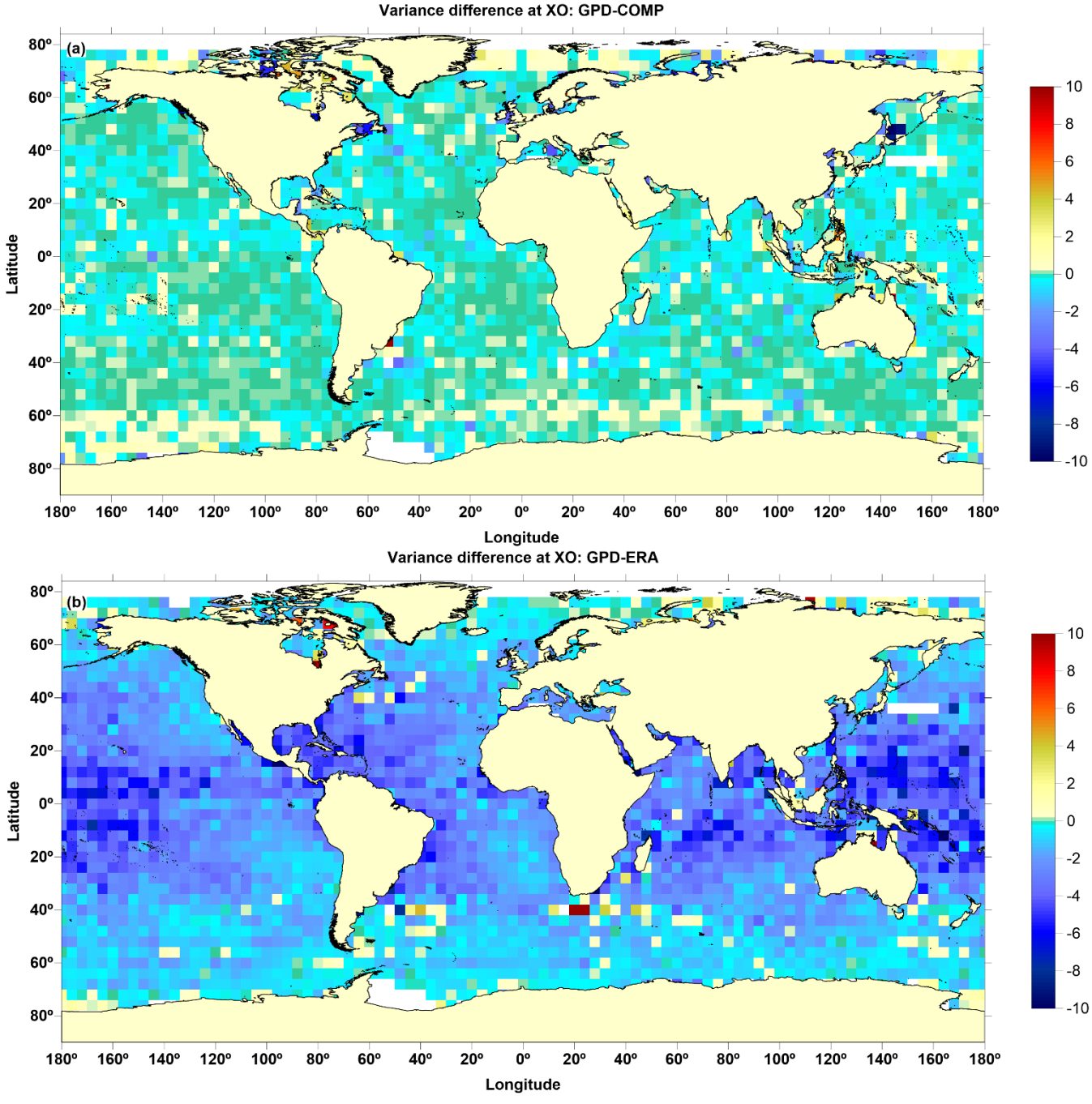

Figure 9 Spatial distribution of the weighted SLA variance differences at crossovers (XO) between (a) GPD+ and the Composite WTCs and (b) GPD+ and the ERA Interim WTCs for the whole Envisat period (cycles 006 to 113).

695

https://doi.org/10.5194/essd-2019-171
Preprint. Discussion started: 17 October 2019

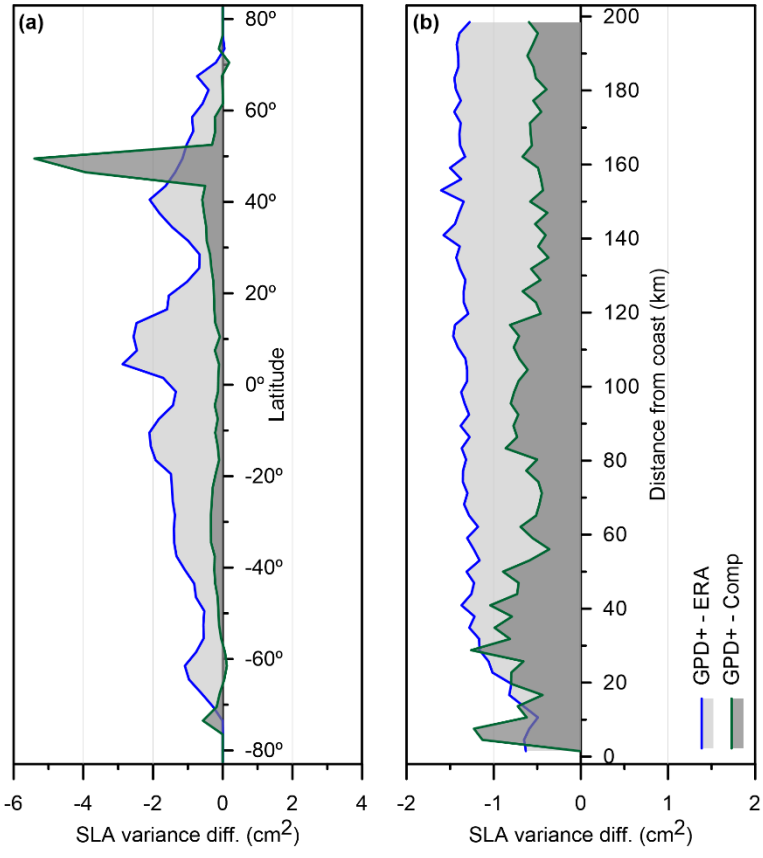

Figure 10 Variance differences of SLA versus latitude (a) and distance from coast (b) between GPD+ and ERA Interim WTCs (blue) and GPD+ and the Composite WTCs (green) for Envisat cycles 006 to 113.

700